Collision of Feigenbaum cascades

G. L. Oppo and A. Politi
Istituto Nazionale di Ottica, Largo Enrico Fermi 6, I-50125 Firenze, Italy
(Received 27 September 1983; revised manuscript received 19 March 1984)

The existence in dynamical systems of chaotic bands delimited on both sides by period-doubling cascades is a general two-parameter phenomenon. Here we show evidence that, whenever these chaotic regions disappear, the bifurcation convergence rate undergoes a slowing down and asymptotically approaches the square root of the universal number $\delta=4.6692\ldots$. A simple renormalization-group analysis is performed to explain this critical behavior and its scaling properties. In particular a theoretical universal function describing the evolution of the convergence rate from $\delta^{1/2}$ to δ is given and numerically verified.

I. INTRODUCTION

A large variety of nonlinear dynamical systems shows a chaotic behavior in given regions of the parameter space. These regions are delimited by different critical phenomena: a sequence of period-doubling bifurcations,[1] intermittency,[2] or crisis.[3]

The existence of chaotic bands delimited on both sides by period-doubling cascades is a quite general phenomenon prevalently associated with the locking of two different frequencies.[4–6] For instance, Contopoulos has recently shown[4] that in one conservative system, a rotating galaxy model, the two cascades may collapse together and reduce to only a finite number of bifurcations, depending on the amplitude of the perturbation. The same phenomenon can be observed in dissipative systems as well: forced Brusselator equation,[5] hydrodynamics,[6] magnetoconvection[7] and optical bistability.[8]

Finally, the existence of inverse cascades has been experimentally observed in an electronic forced oscillator[9] where, moreover, the measured values of the first and second Feigenbaum ratios turned out to be consistently smaller (2.11, 3.31) than the theoretical prediction.

The aim of this paper is to provide a detailed analysis of the critical behavior when the chaotic window disappears, the two cascades collapsing together. The understanding of the underlying physics is reached through a two-parameter study of the phase diagram: the first one to follow the period-doubling cascades, the second one to control the width of the chaotic region. In particular, we show that the collision of cascades is characterized by a slowing down in the convergence rate, which approaches the square root of the Feigenbaum value $\delta=4.6692\ldots$, thus explaining the discrepancy between the standard theory and the experiment of Ref. 9.

More precisely, for any sufficiently small, but nonzero, chaotic window, the first convergence rates δ_n stay close to $\delta^{1/2}$, while at larger n's they asymptotically reach δ. By changing the second parameter ν until the chaotic region disappears ($\nu=\nu_c$), the number of bifurcations showing a rate $\delta^{1/2}$ diverges to infinity. Here we give the theoretical expression for the universal function $\delta_n(\nu-\nu_c)$ which describes the growth of the convergence rate from $\delta^{1/2}$ to δ versus n and $\nu-\nu_c$. Finally, using a renormalization-group technique with a continuous parameter dependence, we interpret the collision of cascades as the simplest of the nonfundamental fixed points recently introduced by Daido.[10]

In Sec. II we perform a numerical analysis of a doubly forced Duffing equation, which shows evidence of collision of cascades. We also measure a critical convergence rate which turns out to be different from the Feigenbaum one. In Sec. III we introduce a cubic map associated in a qualitative way to the differential equation and measure a critical convergence rate equal to the square root of the universal number $4.6692\ldots$. In Sec. IV we go through simple renormalization group (RG) considerations to give a theoretical interpretation of this behavior. In particular, we show how the order of the crossover bifurcations n_c scales versus the difference $\nu-\nu_c$ and give a numerical verification of such a scaling law. In Sec. V we follow a slightly modified version of Daido's approach to study the dependence of a recursive map on the first parameter μ for $\nu=\nu_c$.

II. DOUBLY FORCED DUFFING EQUATION

The sequence of period-doubling bifurcations is perhaps the most common route to chaotic behavior in dynamical systems. A one-parameter study of such a critical phenomenon leads to the discovery of one well-defined transition value μ_∞: the accumulation point of Feigenbaum cascades. If we include in the study the dependence of a second parameter ν there will be, in general, a whole line of critical points $\mu_\infty(\nu)$ separating the ordered from the chaotic phase (see Fig. 1).

Now, depending on the path followed in the phase diagram, we may observe different phenomenologies: a single transition order chaos (OC) (see curve a in Fig. 1), a transition OC followed by a reverse one (curve b), only a finite number of bifurcations (curve c), or, finally, a pointlike chaotic region corresponding to a path tangent to the critical line $\mu_\infty(\nu)$ (curve d).

In order to study this last critical behavior in a differential equation we have preferred to analyze a nonau-

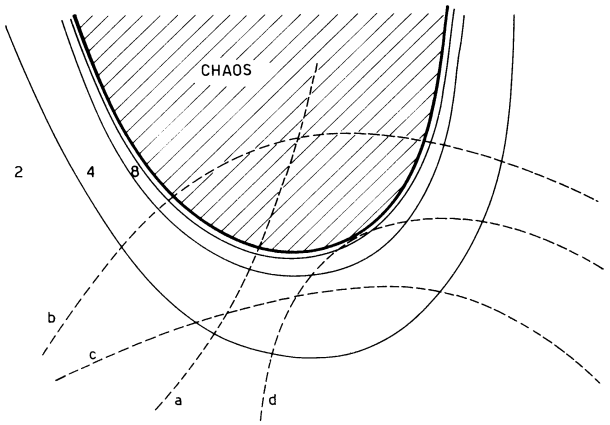

FIG. 1. Two-parameter phase diagram for a generic dynamical system showing a transition to chaos via period-doubling bifurcations. Numbers indicate the periodicity of the solution. Curves represent paths exhibiting different phenomenologies: (a) a single transition order chaos; (b) a transition order chaos followed by a reverse one; (c) no transition to chaotic states; (d) an infinite period-doubling cascade immediately followed by a reverse one (collision).

tonomous system because it offers the possibility of constructing a Poincaré section and measuring the bifurcation points in a very accurate way. Indeed, the return time T to the Poincaré section is preassigned and it is known with a much better accuracy than the other, numerically integrated, variables.

Precisely, we have studied the following Duffing equation:

$$\ddot{x}=-\gamma\dot{x}+x-4x^3+A\cos(\omega_1 t)+B\cos(\omega_2 t)\ , \qquad (1)$$

with $\gamma=0.154$ and $\omega_1=1.17$. If we choose $A=0.09$ and $B=0$, the asymptotic solution of Eq. (1) is periodic with the same frequency as the external force (ω_1) and it is close to the first period-doubling bifurcation (increasing A by a small amount).[11] On the contrary, if we increase B from 0, for many different values of the winding number $W=\omega_2/\omega_1$, we may observe period-doubling cascades immediately followed by reverse ones. In particular, from the data obtained for $W=\frac{2}{5}$ and reported in Table I, we can see that the convergence rate remains considerably different from the Feigenbaum ratio both for the direct and reverse cascade.

In order to gain a better understanding of this phenomenon, we have drawn in Fig. 2 a Poincaré section for a return time $T_1=2\pi/\omega_1$ and $B=0.002\,778\,88$, when the solution is chaotic (the largest Lyapunov exponent being 3.3×10^{-4}). Since the five different pieces making the section lie on simple curves, it is possible to build one-dimensional return maps for any of them. Indeed, once we have chosen piece 1 of Fig. 2 and one of its coordinates (e.g., x axis), the x value of any point on 1, is plotted versus the x value of its previous image, corresponding to a time $5T_1$ earlier, on the same piece.

The resulting map shows the following distincting features: (a) an inflection point where the curvature changes sign, and (b) increasing B essentially corresponds to lower the map (see Fig. 3). We now directly introduce a map sharing the same features of this recurrence numerically built for the Duffing oscillator.

III. THE CUBIC MAP

Let us introduce the cubic map

$$x_{n+1}\equiv f_\mu(x_n)=x_n^3-\nu x_n-\mu \qquad (2)$$

TABLE I. Bifurcation values B_n and convergence rates δ_n of the direct and inverse cascades for the doubly forced Duffing equation (1) with $\gamma=0.154$, $\omega_1=1.17$, $\omega_2=0.468$, and $A=0.09$.

Bifurcation	10^2B_n	$10^2(B_{n+1}-B_n)$	δ_n
5-10	0.248 512 687		
		0.017 110 936	
10-20	0.265 623 623		2.3703
		0.007 218 934	
20-40	0.272 842 557		2.4558
		0.002 939 487	
40-80	0.275 782 043		2.3924
		0.001 228 679	
80-160	0.277 010 722		2.4216
		0.000 507 388	
160-320	0.277 518 110		
320-160	0.278 620 255		
		0.000 460 329	
160-80	0.279 080 584		2.2217
		0.001 022 698	
80-40	0.280 103 282		2.2339
		0.002 284 653	
40-20	0.282 387 935		6.1522
		0.014 055 628	
20-10	0.296 443 562		

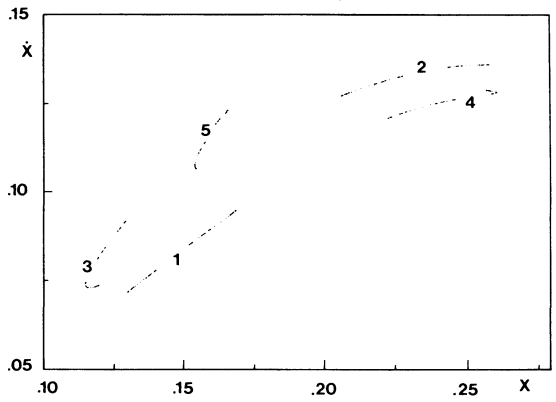

FIG. 2. A Poincaré section for the doubly forced Duffing equation with $B=2.778\,88\times10^{-3}$. The representative point falls in the five regions according to the sequence 1-2-3-4-5-1-2 $\cdots$.

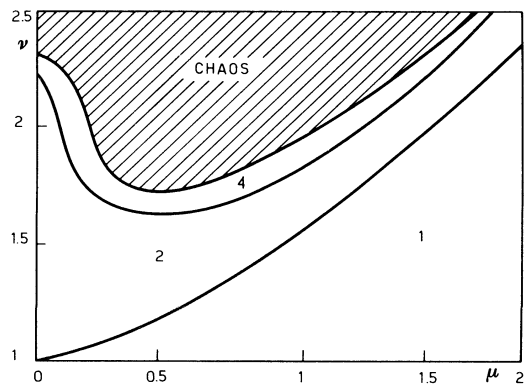

FIG. 4. Phase diagram for the map of Eq. (2); the numbers indicate the periodicity of the solution. Paths corresponding to horizontal straight lines, may intersect the chaotic region depending on ν values.

to investigate in a simpler way the phenomena previously observed for the Duffing equation. The role of the parameters A,B is essentially played now by ν,μ.

Since the recurrence (2) is symmetric under the transformation $(x,\mu)\rightarrow(-x,-\mu)$, we will restrict our analysis to the positive μ's. Indeed for μ smaller than 0 we get the same phenomenology but in inverse order, as for $\mu>0$. If $\mu>\mu_0=(2/3\sqrt{3})(\nu+1)^{3/2}$ there exists only one unstable fixed point x_3. At $\mu=\mu_0$ a pair of stable-unstable fixed points (x_2,x_1) is created via a tangent bifurcation. On further decreasing μ we can observe an entire period-doubling cascade if ν is sufficiently large, or only a finite number of bifurcations if ν is small (see Figs. 4 and 5). For ν ranging between 1.74... and 2.3..., after a chaotic band, an ordered behavior is restored in the region around $\mu=0$. We can easily understand this phenomenon noticing that in this range of parameters there exists an interval around the maximum of $f_\mu(x_n)$ mapped around the minimum and then back into itself. Since the map, close to its extrema, is a contracting one, it is not surprising to find some stable solutions. More importantly, the ordered behavior is restored via a period-doubling cascade, that is to say, the chaotic region is delimited on both sides by period doublings which, depending on ν, may collide. A qualitative explanation of this behavior can be found in the existence of an inflection point of the map; indeed, by increasing the control parameter, the solution, instead of visiting less stable regions, may fall into the more stable section on the right of the inflection point.

Let us go now to study the convergence rate of bifurcations around $\nu=\nu_c=1.742\,821\,997\,236\ldots$ where the chaotic region disappears and the two cascades collapse together. In Fig. 6 we have plotted the ratio

$$\delta_n=(\mu_{n-1}-\mu_n)/(\mu_n-\mu_{n+1}) \tag{3}$$

versus n, where μ_n is the nth bifurcation point, for four

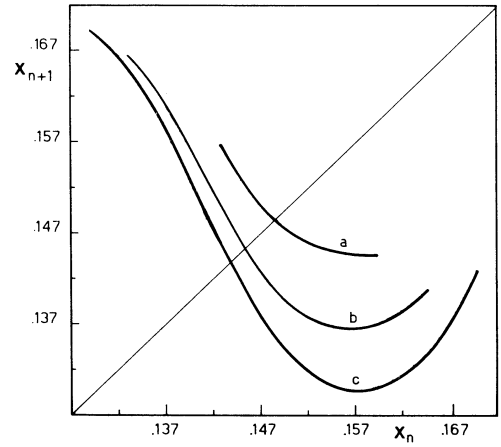

FIG. 3. One-dimensional recursive map built from the Poincaré section for three different values of the control parameter B: (a) $B=2.47\times10^{-3}$ corresponds to a fixed point, (b) $B=2.65\times10^{-3}$ to a cycle of period 2 and (c) $B=2.778\,88\times10^{-3}$ to a chaotic regime.

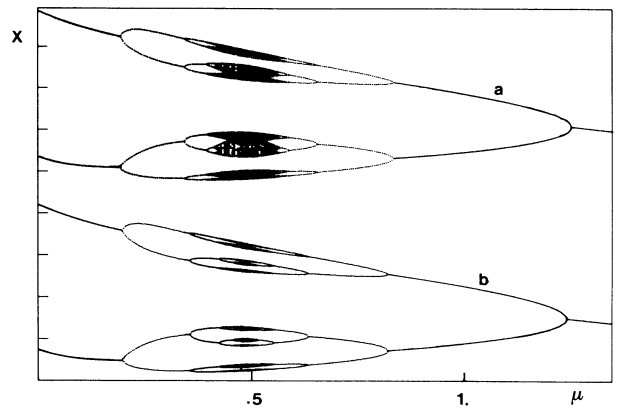

FIG. 5 Bifurcation diagrams for the cubic map (2). For $\nu=1.75$ (a) the two opposite cascades are separated by a chaotic region; for $\nu=\nu_c$ (b) the aperiodic region is reduced to a point-like one.

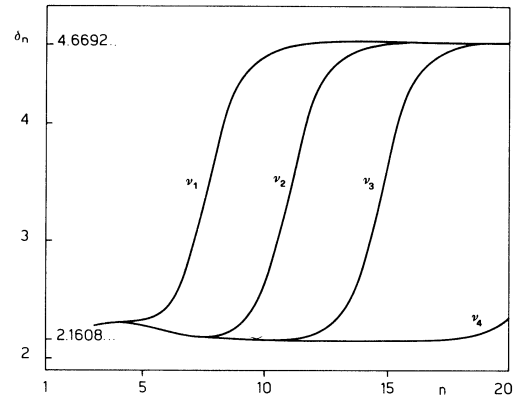

FIG. 6. Convergence rate δ_n vs n for four different ν's: $\nu_1=1.743$, $\nu_2=1.742\,823$, $\nu_3=1.742\,822$, and $\nu_4=1.742\,821\,997\,2361$.

different ν's close to ν_c. We see that if the width of the chaotic region is around 10^{-4} ($\nu=\nu_3$ in Fig. 6) then the rate δ_n reaches the Feigenbaum value after 17 bifurcations. On the other hand, when such a width is less than 5×10^{-6} the rate δ_n remains very close to 2.1608... through all the observed bifurcations, as shown in Table II. In Sec. IV by means of RG considerations, we are able to provide a detailed explanation of the whole subject.

IV. UNIVERSALITY

It is known that the occurrence of a period-doubling cascade in a map is related to the existence of a fixed point f^* of a suitable RG transformation in the functional space of maps.[12] In particular, if the one-parameter family f_μ crosses the stable manifold W_s of f^*, there is a full infinite cascade with a chaotic transition. In order to avoid artificial effects, we should require that the "velocity" $\partial f_\mu/\partial\mu$ in the functional space is everywhere different from zero. This point will, however, be discussed in Sec. V. In Fig. 7 we have sketched the graphic G_f of f_μ for three different ν's. If $\nu=\nu_c$, since the chaotic band is reduced to a pointlike one, G_f is tangent to the stable manifold W_s. Those who are not familiar with such a picture may refer to Fig. 1, where the path followed in the parameter space is essentially equivalent to the graphic G_f of Fig. 7.

Let us denote now with d_n the distance between G_f and W_s; for $\nu=\nu_c$, the generic relation linking d_n and μ_n can be written as

$$d_n=\alpha(\mu_n-\mu_\infty)^2+\beta(\mu_n-\mu_\infty)^3+\cdots\,, \tag{4}$$

where the linear term vanishes according to the previous considerations. If we substitute Eq. (4) into Eq. (3) and recall that d_n scales as δ^{-n},[1,12] we obtain the following asymptotic relation:

$$\mu_n\sim\delta^{-n/2}\,,$$

TABLE II. Bifurcation values μ_n and convergence rates δ_n and δ_n' of the direct and inverse cascades for the cubic map (2) at $\nu=\nu_c$.

n	μ_n	δ_n	δ_n'
1	1.241 622 759 639 4215		
2	0.817 487 591 789 4652	2.275 928 0976	
3	0.631 130 576 254 6814	2.302 572 5243	
4	0.550 196 310 965 0756	2.251 018 3336	1.189 999
5	0.514 241 799 142 3410	2.207 695 4674	1.796 093
6	0.497 955 806 643 8148	2.183 574 8660	2.006 988
7	0.490 497 398 529 6516	2.171 556 5576	2.101 684
8	0.487 062 807 757 5132	2.165 838 1409	2.133 732
9	0.485 477 005 611 3711	2.163 158 1342	2.149 472
10	0.484 743 909 809 9063	2.161 911 3135	2.157 561
11	0.484 404 813 660 6393	2.161 333 4291	2.180 060
12	0.484 247 921 556 5850	2.161 068 3519	2.402 884
13	0.484 175 322 231 3888	2.160 958 0357	
14	0.484 141 726 333 6452		
14	0.484 083 844 542 1932		
13	0.484 050 252 509 4610	2.160 744 1179	
12	0.483 977 665 561 5804	2.160 606 1126	1.967 344
11	0.483 820 835 918 8999	2.160 334 6085	2.142 027
10	0.483 482 031 414 1753	2.159 753 0393	2.163 922
9	0.482 750 297 355 3569	2.158 494 5686	2.171 284
8	0.481 170 853 363 7093	2.155 762 0711	2.184 020
7	0.477 765 947 912 9495	2.149 794 2394	2.198 520
6	0.470 446 101 789 1080	2.136 673 8417	2.230 246
5	0.454 805 978 050 8920	2.107 412 1157	1.689 893
4	0.421 845 791 793 7546	2.057 962 9022	
3	0.354 014 951 225 1242	2.304 570 7604	
2	0.197 693 979 391 0160		

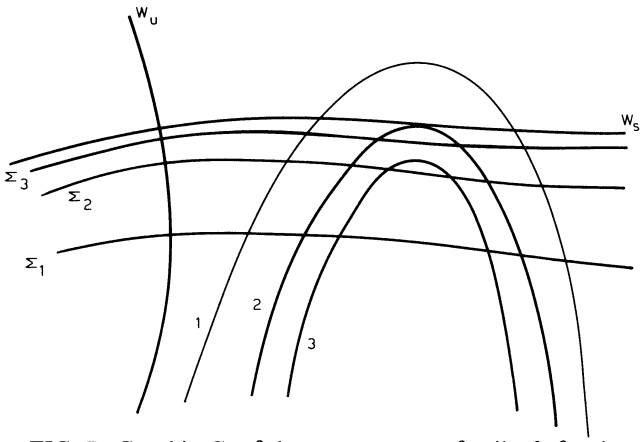

FIG. 7. Graphic G_f of the one-parameter family f_μ for three different ν's in the functional space of the renormalization-group transformations. W_u and W_s represent, respectively, the unstable and stable manifold of the fixed point f^*. Σ_1, Σ_2, and Σ_3 are the surfaces of the superstable maps of periods 2, 4, and 8. By changing μ along curve 1, we can observe two opposite cascades separated by a finite chaotic window. In case 2, the chaotic band reduces to a pointlike one. In 3, the map does not display any bifurcation beyond the second one.

that is to say,

$$\lim_{n\to\infty}\delta_n=\delta^{1/2}\ , \tag{5}$$

in accordance with the data of Table II. Analogously, it is possible to verify that the existence of a nonzero cubic term in Eq. (4) implies that also

$$\delta_n'=\frac{\delta_{n-1}-\delta_n}{\delta_n-\delta_{n+1}} \tag{6}$$

converges to $\delta^{1/2}$, as is again verified in Table II.

Introducing $\bar\nu=\nu-\nu_c$, we see that for $\bar\nu>0$ the graphic G_f intersects twice W_s in the two different accumulation points of the opposite cascades, while for $\bar\nu<0$ no one intersection exists (see Fig. 7). Therefore, for suitable small $\bar\nu>0$ and large enough n, the distance d_n can be written as

$$d_n=a(\bar\nu+b\mu_n^2) \tag{7}$$

neglecting higher-order terms. In this way, the two accumulation points turn out to be $\mu_\infty=\pm(\bar\nu/b)^{1/2}$. By shifting the origin of μ to the positive μ_∞, Eq. (7) becomes

$$d_n=(ab)\left[\bar\mu_n^2+2\left[\frac{\bar\nu}{b}\right]^{1/2}\bar\mu_n\right]\ , \tag{8}$$

where $\bar\mu_n=\mu_n-\mu_\infty$. Since the distance d_n scales as δ^{-n}, we obtain

$$\bar\mu_n=(ab)^{1/2}[-(a\bar\nu)^{1/2}+\delta^{-n/2}F(a\bar\nu\delta^n)]\ , \tag{9}$$

where

$$F(x)=\sqrt{1+x}\ . \tag{10}$$

The convergence rate is consequently given by

TABLE III. Comparison between the theoretical predictions of δ_n from Eq. (11) and the numerical data evaluated on the cubic map (2) at $\nu=1.742\,822$.

n	Theoretical δ_n	Numerical δ_n
9	2.161 25	2.166 25
10	2.162 77	2.165 10
11	2.169 83	2.179 01
12	2.201 90	2.202 40
13	2.335 55	2.335 77
14	2.764 58	2.764 66
15	3.575 75	3.575 75
16	4.284 31	4.284 31
17	4.572 38	4.572 46

$$\delta_n(\bar\nu)=\frac{\delta^{1/2}F(\bar\nu\delta^{n-1})-F(\bar\nu\delta^n)}{F(\bar\nu\delta^n)-\delta^{-1/2}F(\bar\nu\delta^{n+1})}\ , \tag{11}$$

where the dependence on a has been removed by using an arbitrary scale for $\bar\nu$. Once we have chosen a $\bar\nu$ small enough, we can recognize two different regimes: small and large n corresponding to $x(\equiv\bar\nu\delta^n)\ll 1$ and $x\gg 1$, respectively. In the former case δ_n is close to $\delta^{1/2}$ because $F(x)\sim 1$; in the latter one δ_n approaches δ because $F(x)\sim x^{1/2}+x^{-1/2}/2$.

To test Eq. (11), let us first come back to Fig. 6 where the curves look very much as shifted versions of the same universal curve. This is indeed the case, as it is evidenced in Eq. (11), where the dependence on $\bar\nu$ and n is entirely contained in the product $\bar\nu\delta^n$. Consequently, a simple scaling law can be inferred: any change of $\bar\nu$ from a fixed reference value can be naturally compensated by a shift in the bifurcation order n

$$n=\frac{-\ln\bar\nu}{\ln\delta}+C\ , \tag{12}$$

where C is an unessential constant. Therefore, by fitting the *a priori* unknown horizontal shift, it has been possible to compare the theoretical predictions of Eq. (11) with the numerical values gotten for $\nu=1.742\,822$. The data of Table III show a good agreement (the first four figures coincide) in the crossover region where δ_n changes from $\delta^{1/2}$ to δ. The larger discrepancy at small n's is due to the neglected higher-order terms.

To verify now the scaling law (12), we choose at first an intermediate value $\bar\delta$ between $\delta^{1/2}$ and δ, and then associate to each $\bar\nu$ the corresponding bifurcation order n such that $\delta_n(\bar\nu)=\bar\delta$. To do this, we interpolate the numerical data through Eq. (11), giving formal meaning even to noninteger n's. We report in Fig. 8 n versus $\ln\bar\nu$ for a choice of $\bar\delta=3$. The points are well aligned on a straight line with a measured slope 0.650 very close to theoretical prediction $1/\ln\delta=0.6489\ldots$.

So far we have discussed the case of infinite sequences of bifurcations when a chaotic region still exists. Now, let us turn our attention to the finite case. It is readily seen that Eq. (11) holds even for $\bar\nu<0$, i.e., beyond the collision, and it is also possible to evaluate the number of occurring bifurcations, by looking for the change of sign in the argument of the square root in Eq. (10). Indeed, a

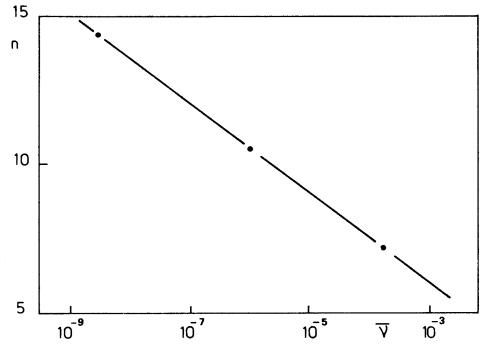

FIG. 8. Numerical evidence of the scaling law (12) between the order of the crossover bifurcation n and the distance $\bar{\nu}\equiv\nu-\nu_c$. Points correspond to a measure performed on the cubic map (2) for $\nu=\nu_1$, ν_2, and ν_3 as in Fig. 6. Straight line represents the theoretical curve.

negative sign in the square root corresponds to a nonreal value of μ_n for the respective bifurcation. Therefore, by imposing

$$\bar{\nu}\delta^n=-1 \tag{13}$$

and solving for n, we get the requested value for the last bifurcation. Hence $\bar{\nu}<0$ gives rise to a different class of finite curves showing a rate $\delta_n(\bar{\nu})$ always decreasing for increasing n and less than $\delta^{1/2}$ [see Fig. 9, where two theoretical samples of the different classes ($\bar{\nu}<0$ and $\bar{\nu}>0$) have been plotted].

Finally, let us calculate the smallest measurable rate δ_s corresponding to the last bifurcation. By substituting $\bar{\nu}\delta_s^{n+1}=-1$ into Eq. (11), we obtain, after a few algebraic calculations,

$$\delta_s=\sqrt{\delta+1}-1=1.3810\ldots . \tag{14}$$

We can now conclude that, until the measured rate remains close to $\delta^{1/2}$ it is not possible to decide whether the cascade is finite or infinite. Only when we begin to observe an increasing (towards 4.6692...) or decreasing

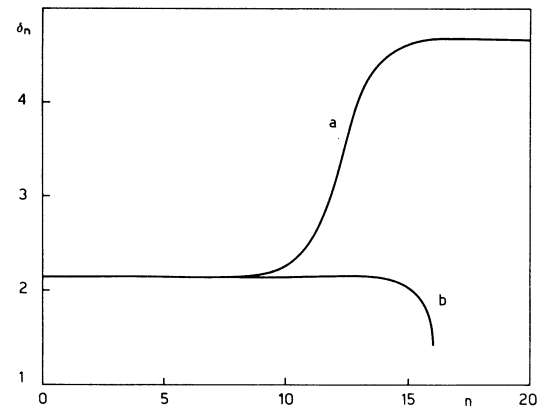

FIG. 9. Universal function $\delta_n(\bar{\nu})$ vs n for two different $\bar{\nu}$'s: $\bar{\nu}>0$ corresponding to an infinite cascade (curve a), and $\bar{\nu}<0$ to a finite sequence of bifurcations.

(towards 1.3810...) tendency can we reach a conclusion in a definite way. In particular, coming back to the results gotten for the differential equation in Sec. II it is apparent that the high-order terms [referring to the expansion (4)] are still non-negligible at the last measured bifurcation, since the behavior of δ_n cannot be described in terms of the function (11). Anyway, we can reasonably assume that, being $\delta_n>\delta^{1/2}$, a chaotic window exists. In fact, we recall that for a suitable value of B (0.002 778 88), the largest Lyapunov exponent is positive, thus yielding a chaotic behavior.

V. THE RENORMALIZATION-GROUP ANALYSIS

We now describe the collision of Feigenbaum cascades in terms of a generalized version of the RG approach contained in Ref. 1. Since we are not only interested in the dependence on the dynamical variable x, but also in the scaling respect to the parameter μ, it is more convenient to follow a slightly modified version of the RG scheme introduced by Daido.[10]

Let us start with a one-parameter family of maps on the interval (0,1)

$$x_{n+1}=f_\mu(x_n) \tag{15}$$

and rescale both the variable x and the parameter μ. Namely, x is transformed according to

$$z=\frac{x-x_n^*(\mu)}{x_n^*(\mu)-x_{n-1}^*(\mu)}\ , \tag{16}$$

where x_n^* belongs to the 2^n-periodic orbit and is chosen with a fixed rule between the two points bifurcating from x_{n-1}^* at $\mu=\mu_{n-1}$. On the other hand, differently from Daido, let us rescale μ as

$$y=\frac{\mu-\mu_\infty}{\mu_n-\mu_\infty} \tag{17}$$

thus allowing a clear-cut interpretation of the so-called nonfundamental fixed points, as we will see in the following.

We can now introduce the RG transformation

$$G_n(z,y)=\frac{f^{2^n}(x(z,y))-x_n^*(y)}{x_n^*(y)-x_{n-1}^*(y)} \tag{18}$$

whose fixed-point equations are

$$\begin{aligned} G(z,y)&=\frac{1}{\epsilon(y)}G^2(\epsilon(y)(1+z),\delta^{-1}y)\ ,\\ \epsilon(y)&=G^2(\epsilon(y),\delta^{-1}y)\ , \end{aligned} \tag{19}$$

where $\epsilon(y)$ is the asymptotic rescaling factor of the variable x

$$\epsilon(y)=\lim_{n\to\infty}\frac{x_n^*(y)-x_{n-1}^*(y)}{x_{n-1}^*(y)-x_{n-2}^*(y)} \tag{20}$$

analogous to the $\alpha=2.5029\ldots$ of Ref. 1. By introducing the Taylor expansion of $G(z,y)$ with respect to the spatial variable z,

$$\lambda^{(i)}(y)\equiv\frac{\partial^i}{\partial z^i}G(z,y)\,|_{z=0}\,, \tag{21}$$

we can formally rewrite Eqs. (19) as

$$\underline{\lambda}(y)=\underline{L}(\underline{\lambda}(\delta^{-1}y))\,. \tag{22}$$

The Feigenbaum theory shows the existence of a fixed point $\underline{\lambda}(y)$ with a relevant eigenvalue $\delta=4.6692\ldots$. Let us now introduce the following transformation on the parameter y:

$$\tau_m(y)\equiv y^m \tag{23}$$

which leaves unchanged the accumulation point in $\tau_m=0$ and the first bifurcation ($y=1$) in $\tau_m=1$ in accordance with the definition (17). By substituting y with τ_m in Eq. (22), we immediately see that $\underline{\lambda}(\tau_m(y))$ is again a fixed point with relevant eigenvalue

$$\hat{\delta}=\delta^{1/m}\,. \tag{24}$$

The nonfundamental fixed points ($m>1$) have now a direct interpretation: looking at Eq. (23), we can simply notice that m corresponds to the multiplicity of the crossing point between the graphic G_f and the stable manifold W_s (see, for instance, Fig. 7 or, for simplicity, Fig. 1 referring to a path in the parameter space instead of to G_f). Hence, the collision of cascades, being characterized by a tangency, can be associated to a fixed point with $m=2$ and eigenvalue $\delta^{1/2}$.

It is worthwhile to notice that a trivial way to get an eigenvalue $\delta^{1/m}$, for any arbitrary choice of m, is to shift the zero of μ to μ_∞ and rescale $\bar{\mu}$ according to Eq. (23). Therefore, in such cases, the graphic G_f is not distorted from a transversal (with respect to W_s) into a tangent one, but more simply, the "velocity" along the curve G_f is modified. This is exactly the case mentioned in the previous section when, changing the parametrization, we obtain $\partial f_{\bar{\mu}}/\partial\bar{\mu}=0$ for $\bar{\mu}=0$. This result is a purely artificial one and it can be clearly evidenced by measuring the "rate of the rates" δ'_n [see Eq. (6)] which, different from δ_n, remains equal to $4.6692\ldots$. Indeed, if we transform $\bar{\mu}\to\bar{\mu}^m$ in Eq. (4), we obtain a peculiar expansion where only the powers which are multiples of m are present. In particular, the absence of the $(m+1)$th power implies that δ'_n asymptotically converges to δ. This is not the case of the cubic map (2) for which the δ'_n values turn out to be very close to $\delta^{1/2}$ (see Table II).

Still following the procedure of Ref. 10 it is possible to evaluate the first terms of $\underline{L}(\underline{\lambda}(y))$ by suitably expanding

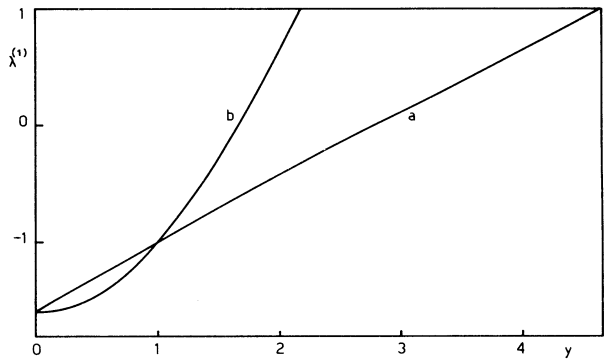

FIG. 10. Stability coefficient $\lambda^{(1)}$ of a periodic orbit vs the rescaled parameter y for a standard Feigenbaum sequence (curve a) and for the collision of two cascades (curve b).

$\epsilon(y)$ in the neighborhood of $y=\delta$. Thus, up to the second order in $(y-\delta)$, we obtain

$$\lambda^{(1)}(\tau_m(y))=1+\frac{16(y^m-\delta)}{(\delta-1)(\delta+4)}-\frac{2(\delta-4)(y^m-\delta)^2}{(\delta-1)^2(\delta+4)}\,. \tag{25}$$

We recall that, from the definition (21), $\lambda^{(1)}$ is the derivative of f_μ along the 2^n-periodic orbit in the limit of large n's; hence, Eq. (25) shows how the stability coefficient of the solution evolves from 1, for $y=\delta^{1/m}$, to the asymptotic value at the accumulation point $y=0$. In Fig. 10 we have reported the theoretical values of $\lambda^{(1)}(y^m)$ for $m=1$ and 2. We have also performed a numerical calculation of $\lambda^{(1)}$ for the cubic map at $\nu=\nu_c$ for which, in spite of the approximations contained in Eq. (25), the difference between theory and direct calculations is always less than 0.5% and could not be appreciated in curve b of Fig. 10. Finally, we conclude by again affirming the generality of the phenomenon so far discussed that occurs in many nonlinear dynamical systems where it is possible to control at least two external parameters.

ACKNOWLEDGMENTS

We wish to thank Dr. S. Ruffo and Professor J. P. Eckmann for helpful discussions and Professor F. T. Arecchi for his kind interest in our work. This work was partially supported by the contract CNR-INO.

[1]M. J. Feigenbaum, J. Stat. Phys. **19**, 25 (1978); **21**, 669 (1979).
[2]Y. Pomeau and P. Manneville, Commun. Math. Phys. **74**, 189 (1980); Physica **1D**, 219 (1980).
[3]C. Grebogi, E. Ott, and J. A. Yorke, Phys. Rev. Lett. **48**, 1507 (1982); Physica **7D**, 181 (1983).
[4]G. Contopoulos, Lett. Nuovo Cimento **37**, 149 (1983).
[5]K. Tomita, Phys. Rep. **86**, 113 (1982).
[6]V. Franceschini, Physica **6D**, 285 (1983).
[7]E. Knobloch and N. O. Weiss, Physica **9D**, 379 (1983).
[8]P. Mandel and R. Kapral, Opt. Commun. **47**, 151 (1983).
[9]J. Cascais, R. Dilão, and A. Noronha da Costa, Phys. Lett. **93A**, 213 (1983).
[10]H. Daido, Phys. Lett. **83A**, 246 (1981); Prog. Theor. Phys. **67**, 1698 (1982).
[11]F. T. Arecchi, R. Badii, and A. Politi (unpublished).
[12]For a more detailed explanation of this terminology, see P. Collet and J. P. Eckmann, *Iterated Maps on the Interval as Dynamical Systems* (Birkhäuser, Boston 1980).